

A tsunami swept over the coasts of the Java and Sumatra islands (Indonesia) on both sides of the [Sunda Strait](#) on Saturday, December 22, 2018 at approximately 9:30 pm (14:30 UTC) causing severe casualties. This tsunami has been caused by a landslide of a low part of the volcanic cone and the collapse of the [Krakatau volcano](#) (also called Krakatau).

Satellite imagery can extensively be used for the follow-up of volcanic eruptions, especially [Sentinel-1](#) radar images for which clouds and plumes are almost transparent and are very sensitive to the morphology, to roughness variations of the land or sea surface. The revisiting time is short, depending on the -use of two satellites S1A and S1B (same orbit with 6 days dephasing), -descending and ascending orbits acquisitions, and -large swath of 240 km in default IW mode.

- The left column of figures 1 and 2 includes radar images. The C-SAR instrument on-board Sentinel-1 is an active radar; i.e. it emits the microwave light at day (descending orbit in fig.1a) and at night (ascending orbit in fig.1c). This directional illumination crosses the clouds, reveals relief particularly well and illuminates brighter the exposed faces of the volcanic cone.
- The right column shows [Sentinel-2](#) images acquired by a passive instrument in the optical domain. When it is not obstructed by clouds, it is therefore the backscattered light of the Sun that is measured in 13 spectral bands ranging from RGB to near and medium infrared.

Tsunami in Sunda strait between Java and Sumatra

[2D_stack](#)

Sentinel-1 (radar) vs. Sentinel-2 (optical)

Fig.1: Sentinel-1 radar (left) and Sentinel-2 optical (right) before the tsunami (a,b) and after (c,d). - View of full scenes and tiles.

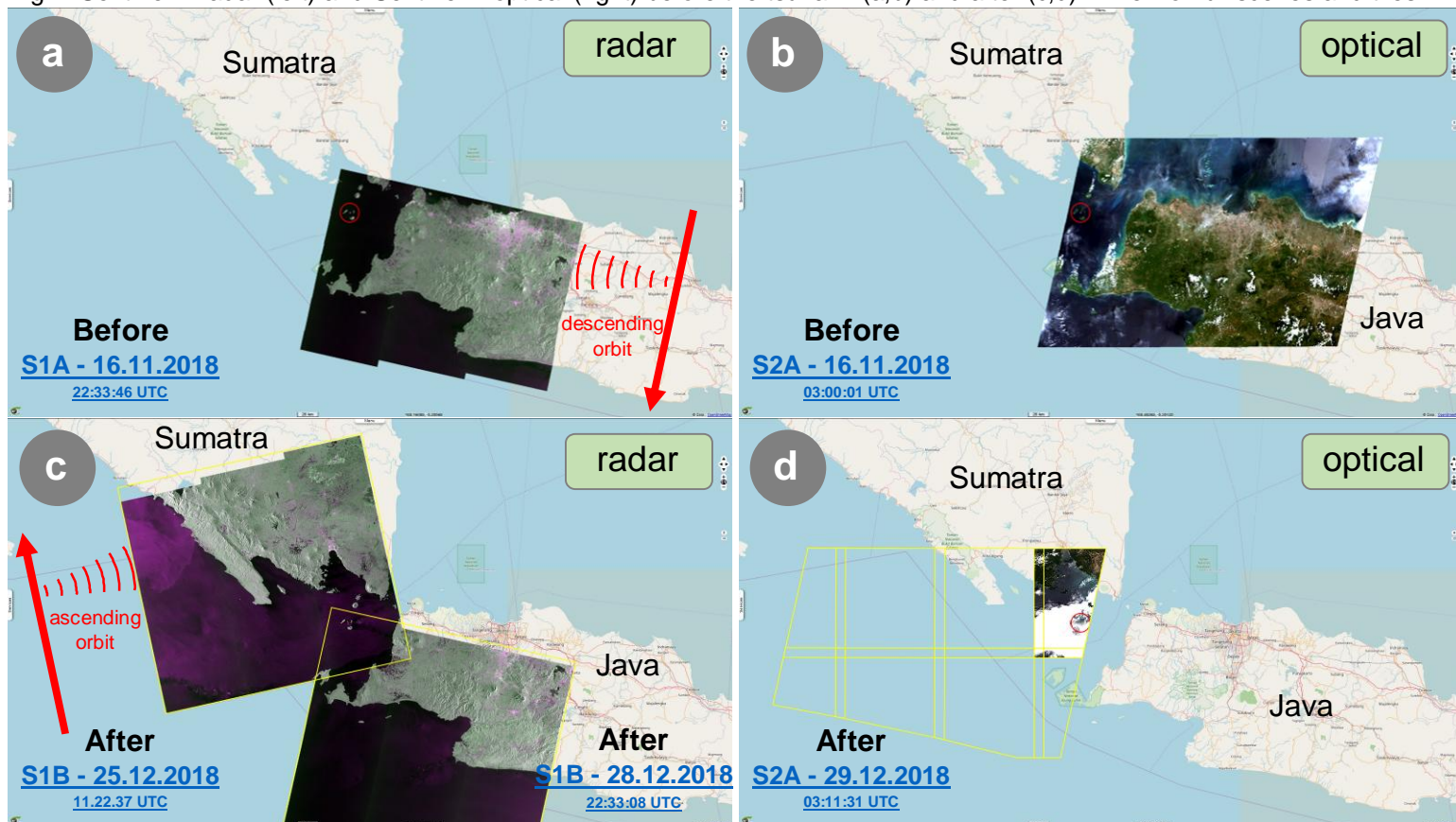
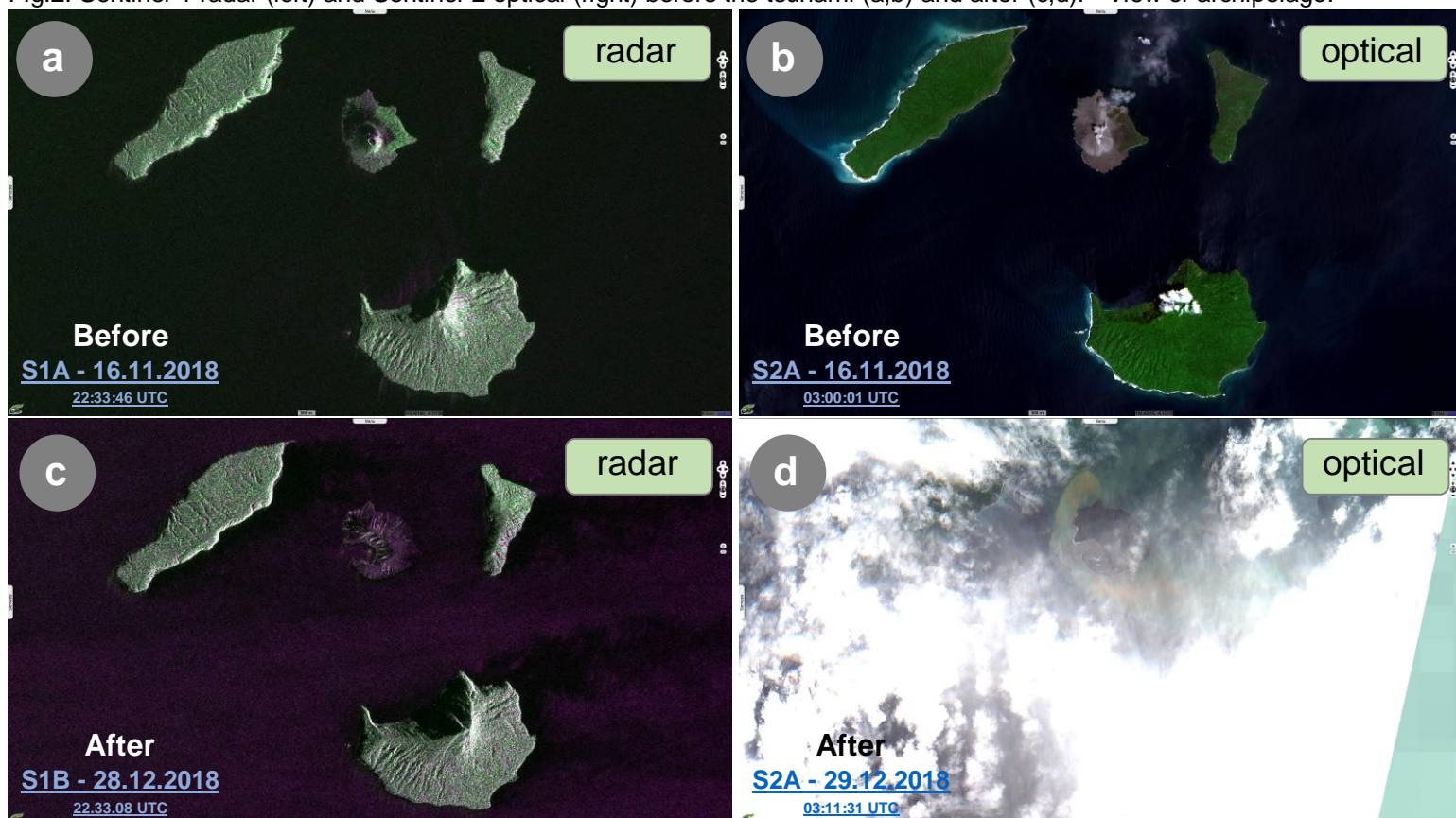


Fig.2: Sentinel-1 radar (left) and Sentinel-2 optical (right) before the tsunami (a,b) and after (c,d). - View of archipelago.



Images in the left column of fig.3 correspond to the radar acquisitions of [Sentinel-1](#) while those in the right column are images acquired in the optical domain by [Sentinel-2](#). The first line (fig.3a and fig.3b) corresponds to observations before the tsunami of December 22, 2018 and those of the second line (fig.3c and fig.3d) to later observations.

The relief revealed by the radar imagery makes it possible to precisely delimit the contours of the crater: -main and adventitious craters (fig. 3a) and -very enlarged crater after the eruption (fig.3c). The colour composition VV,VH,VV shows that the dominant polarization is VH in the vegetated part in the east of the island. The dominant magenta shows the predominance of VV, a sign of a low depolarization over a rough surface of rocks.

The colour composition 12,8,4 used in fig.3b involves the SWIR (shortwave infrared), NIR (near infrared) and the red. The SWIR component (B12) reveals hot-spots in the crater and some isolated points south of the cone of the volcano.

The colour composition 12,3,2 used in fig.3d is the one that minimizes the obstruction of the clouds and smoke at best. Once again, the SWIR band (B12) is used to locate hot-spots around the crater.

Sentinel-1 vs. Sentinel-2

Change of the coastline

Enlargement of the crater

Fig.3: Sentinel-1 radar (left) and Sentinel-2 optical (right) before the tsunami (a,b) and after (c,d). - View of Anak Krakatau island.

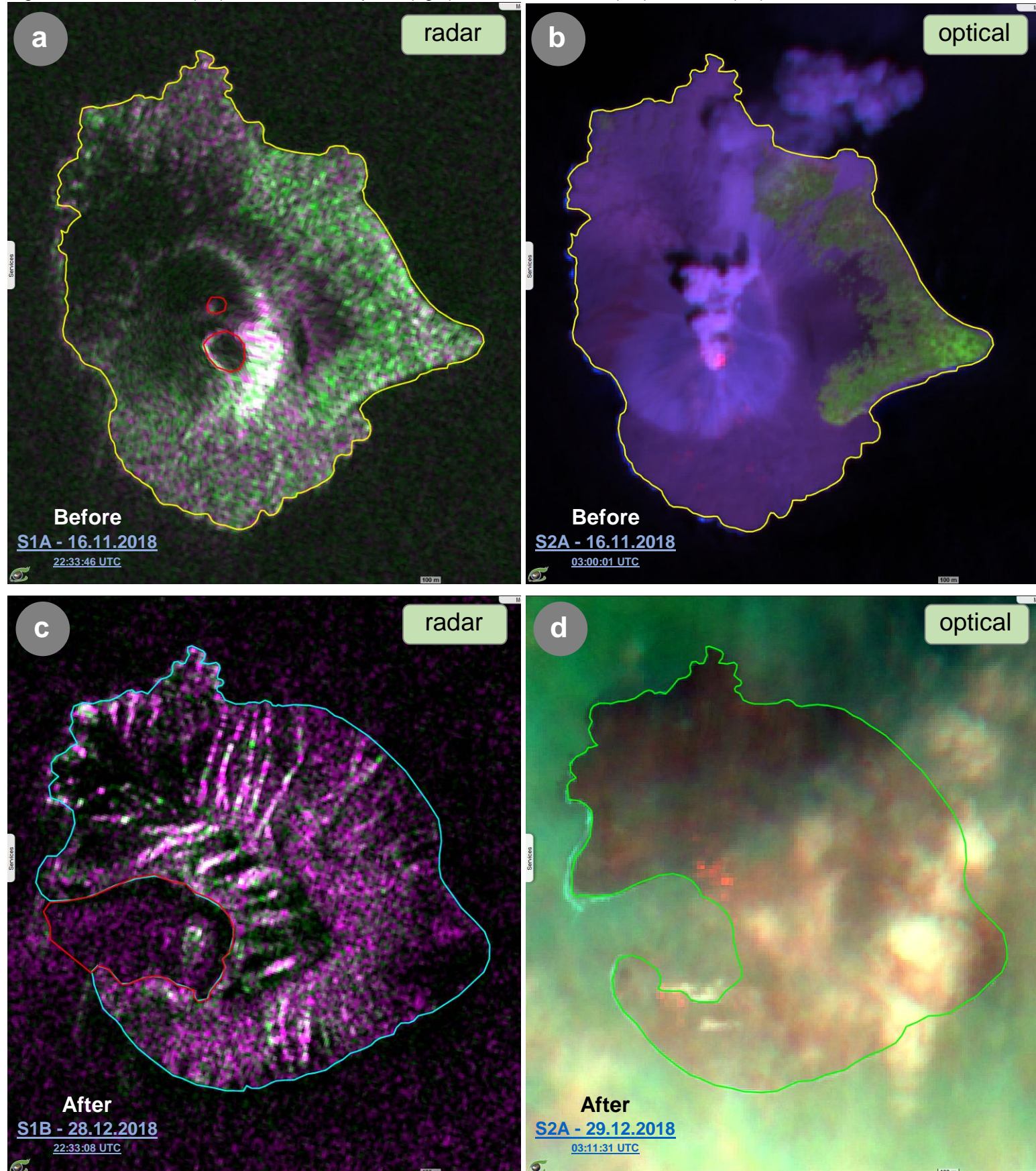


Image 4.a has been acquired 8 hours after the tsunami. In the western part of the island, one can clearly see the lack of a large part of the coast (white polygon). This area is most likely the upper part of the landslide that caused the tsunami.

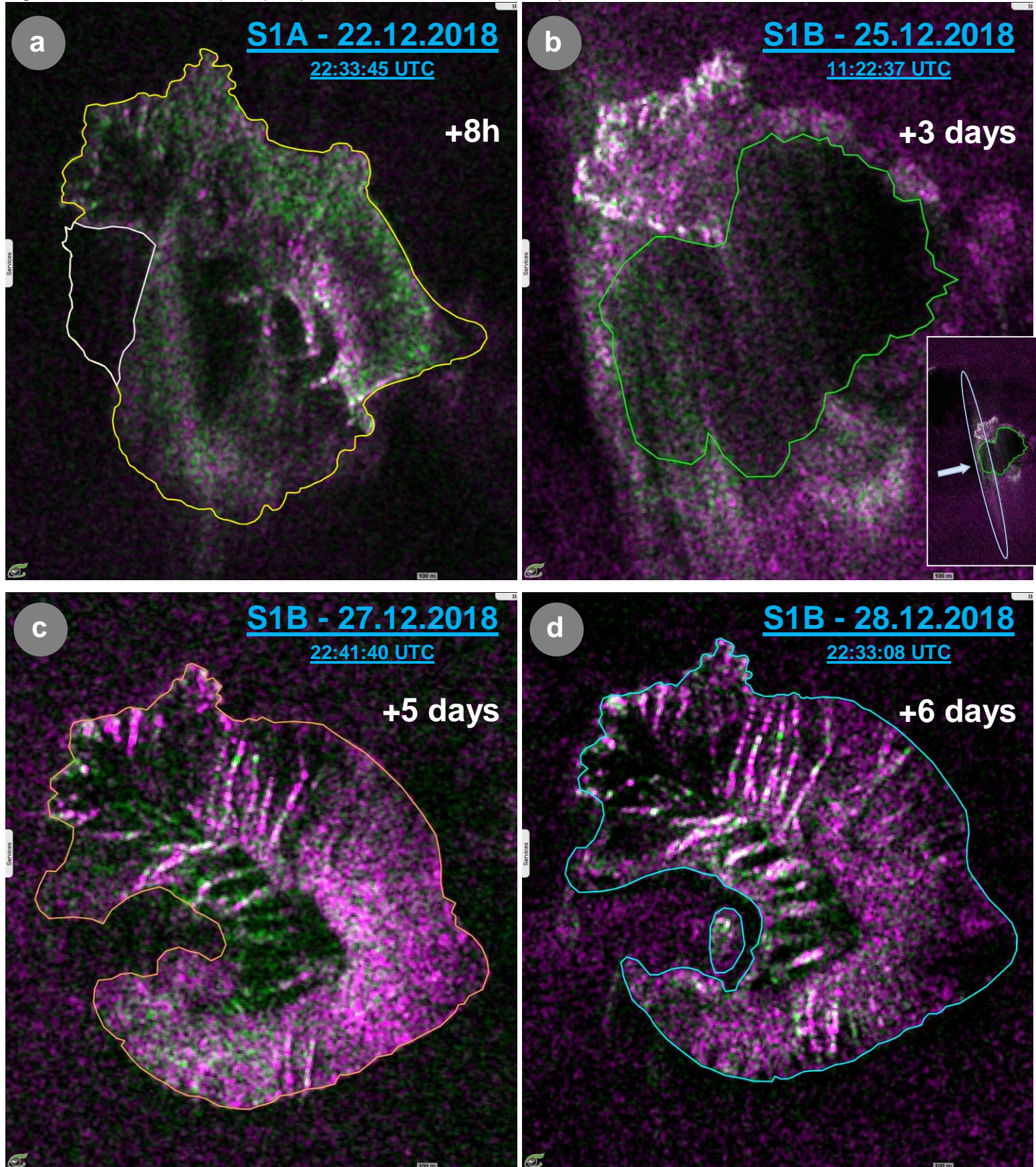
Figure 4.b is blurred. A high density plume, forming a dark mass above the crater suggests that the signal has encountered large targets, probably rocks much larger than the 5.5 cm radar wavelength of the C-band. This material, violently projected vertically, may have produced a Doppler effect that is rendered by the lighter segments (see the blue ellipse perpendicular to the pulse direction being represented by an arrow in the thumbnail). Experts in radar signal processing would certainly estimate the ejection speed from this Doppler effect.

As illustrated in fig.4c and confirmed in fig. 4d, a larger crater of explosion is now present on the west side, while the accumulation of volcanic ejecta expanded to accrete the coast in its eastern part.

Fig. 4d also shows the emergence of an island in the flooded part of the new crater.

Sentinel-1 (HR radar) High temporal resolution time-series of events

Fig.4: Series of Sentinel-1 (radar) acquisitions in the few hours and days after the tsunami event.



The 3D view of radar scene [Sentinel-1](#) (fig.5b) shows the collapsed area that may have caused the tsunami. The whole island did not move down for the coastline before and after is the same everywhere except in the collapsed area.

This 3D view uses the digital terrain model [SRTM](#) acquired in February 2000 and it is very likely that this DEM is now obsolete for "Anak Krakatau" island ("Child of Krakatau") that emerged in 1927. The image acquired on 22 December 2018 is the last one in the present study that uses the VtWeb orthorectification. Images acquired after this date are simply mapped on the WGS84 ellipsoid. The difference between these two geocoding techniques is illustrated in this [animation](#).

The radar scene dated 22.12.2018 at 22:33:45 UTC was acquired exactly **8 hours** after the onset of the tsunami. The top figure is an average of the previous 4 Sentinel-1A scenes with a 12-days (revisit) cycle in descending orbit. The colours exploit the two polarizations VV and VH of the C-SAR instrument.

Sentinel-1 on 22.12.2018 8 hours after the tsunami Collapse of the volcano

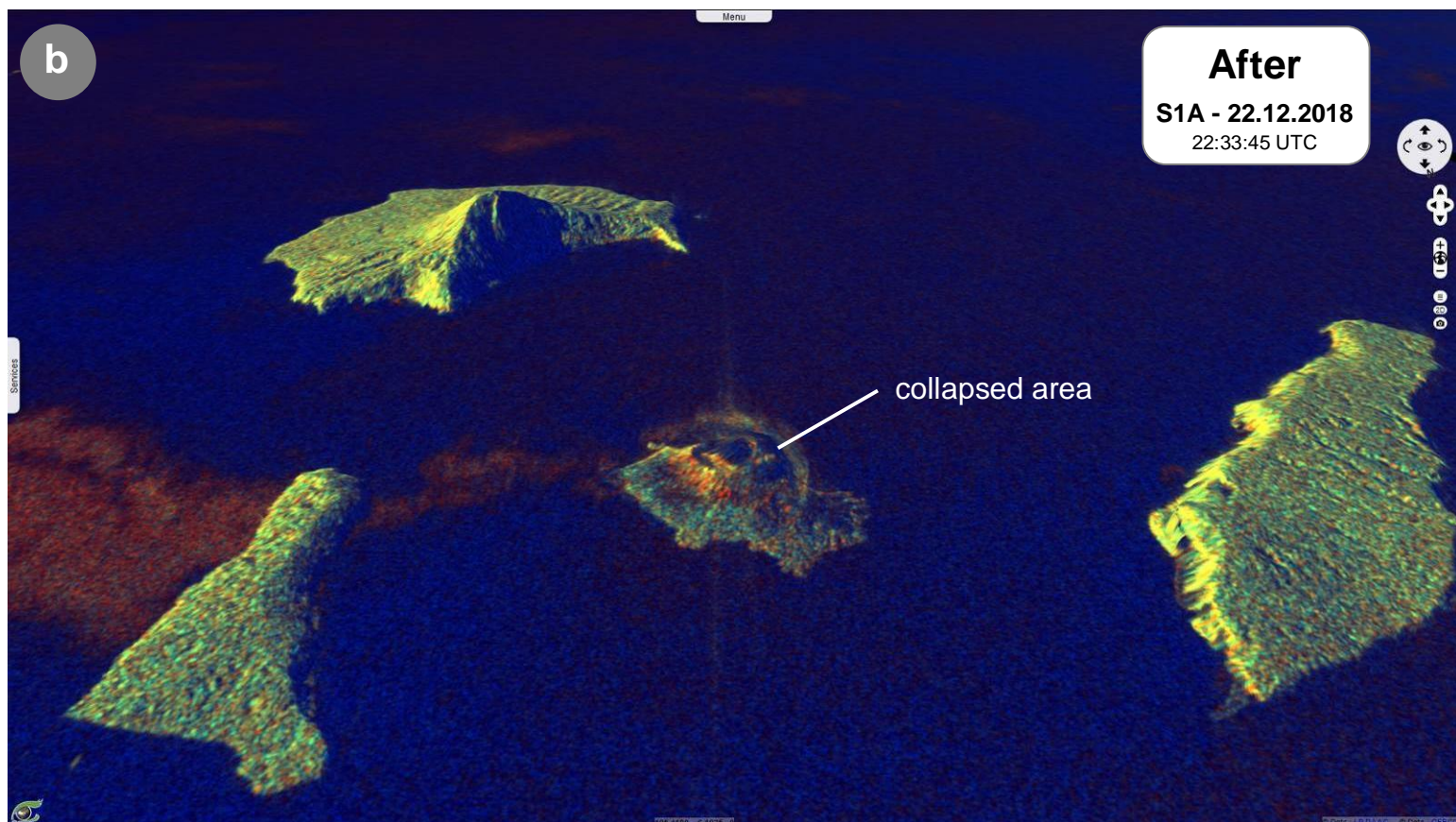
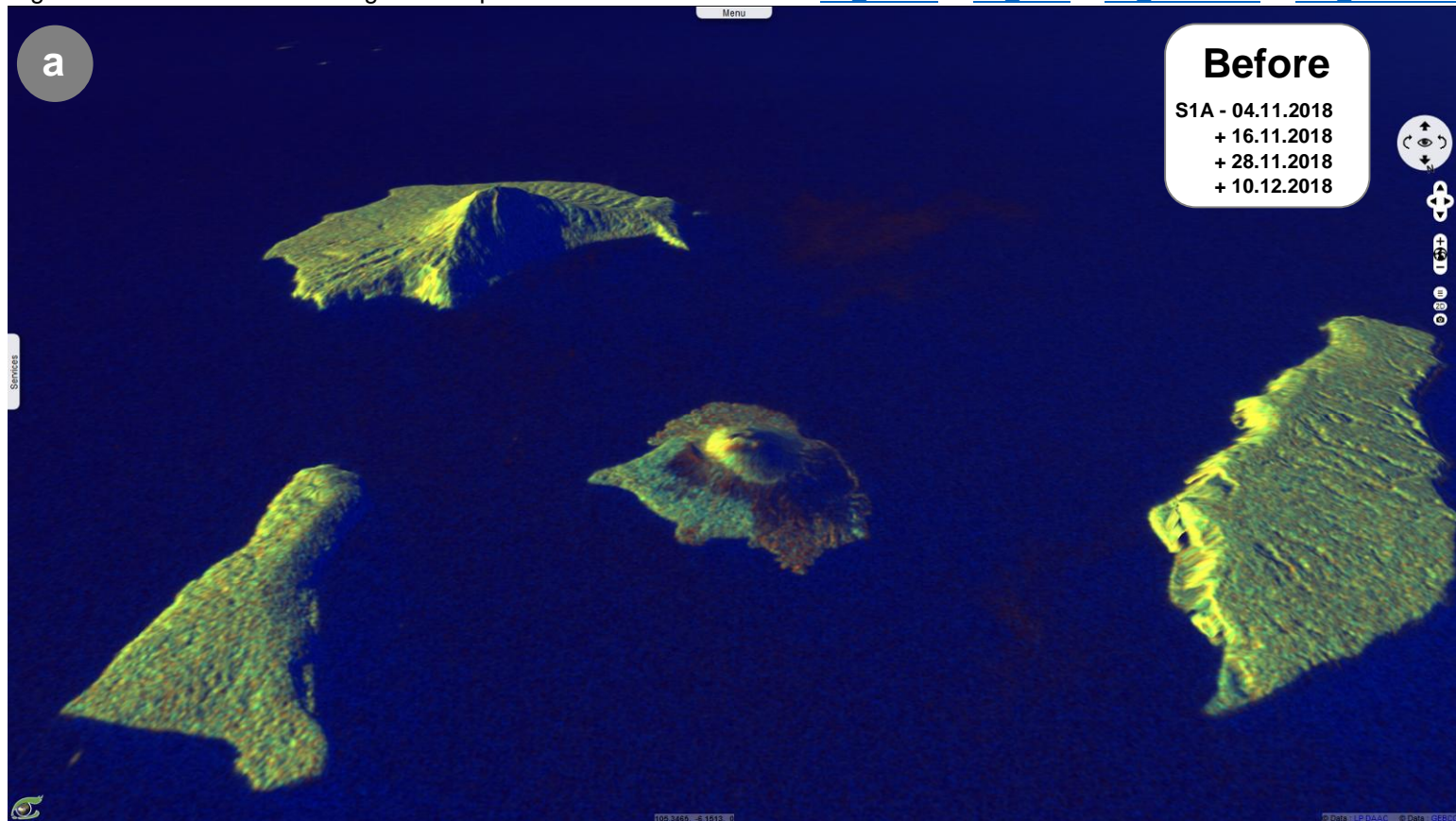
Fig.5: Sentinel-1 scenes showing the collapse of Krakatau volcano.

[3D before](#)

[3D after](#)

[3D animation](#)

[GIF animation](#)



According to Professor Jean Chorowicz, the plume observed on December 22, 2018 in the radar image (fig.6) is not the atmospheric plume itself for it does not show-up over the Panjang island and clouds of water or micro-particles are almost transparent to radar. The sea surface is rough under the panache because the rock fragments that were vertically projected up, felt-down according to their size, the bigger (lava bombs, big fragments) over the volcanic cone they construct, others (lapillis, large cinder particles), drag by wind farther east in the sea were they are responsible for rough sea surface and consequently higher radar backscatter (see explanations in fig.7). Farther east, micro-particles do not fall and the effect of panache is not visible in the radar image.

According to its effects on the sea surface, this plume is eastwardly carried by the winds as confirmed by the [ECMWF](#) Surface Wind Model values set at midnight that same day. The model of ocean surface currents produced by the Copernicus Marine Service ([CMEMS](#)) is directed to the northeast and contributes to the drift of the roughed sea surface.

Sentinel-1 on 22.12.2018 8 hours after the tsunami Heavy plum falling in the sea

Fig.6: Sentinel-1 acquired on 22 December 2018, wind field (cyan) and ocean currents (red).

[2D view](#)

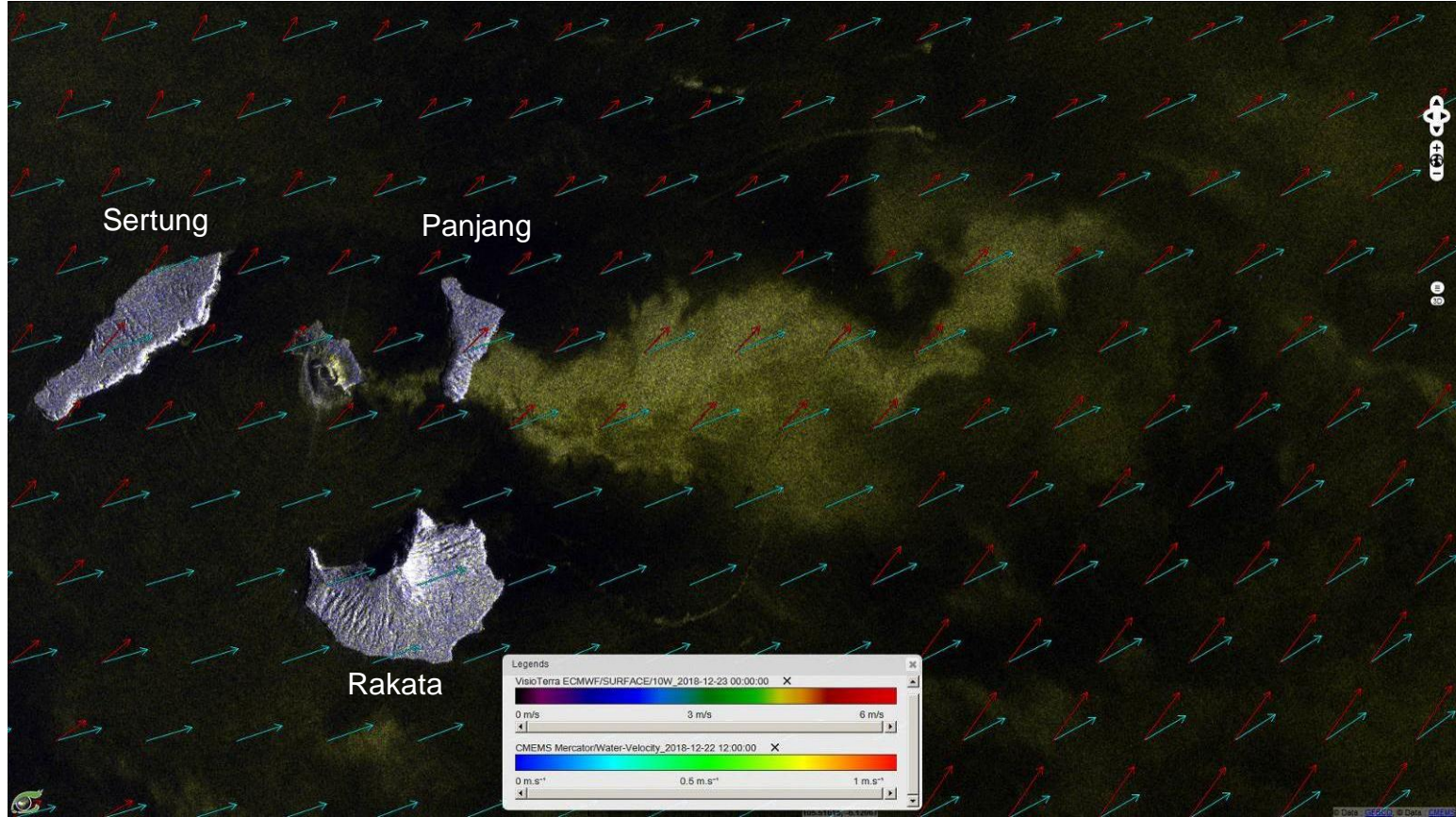
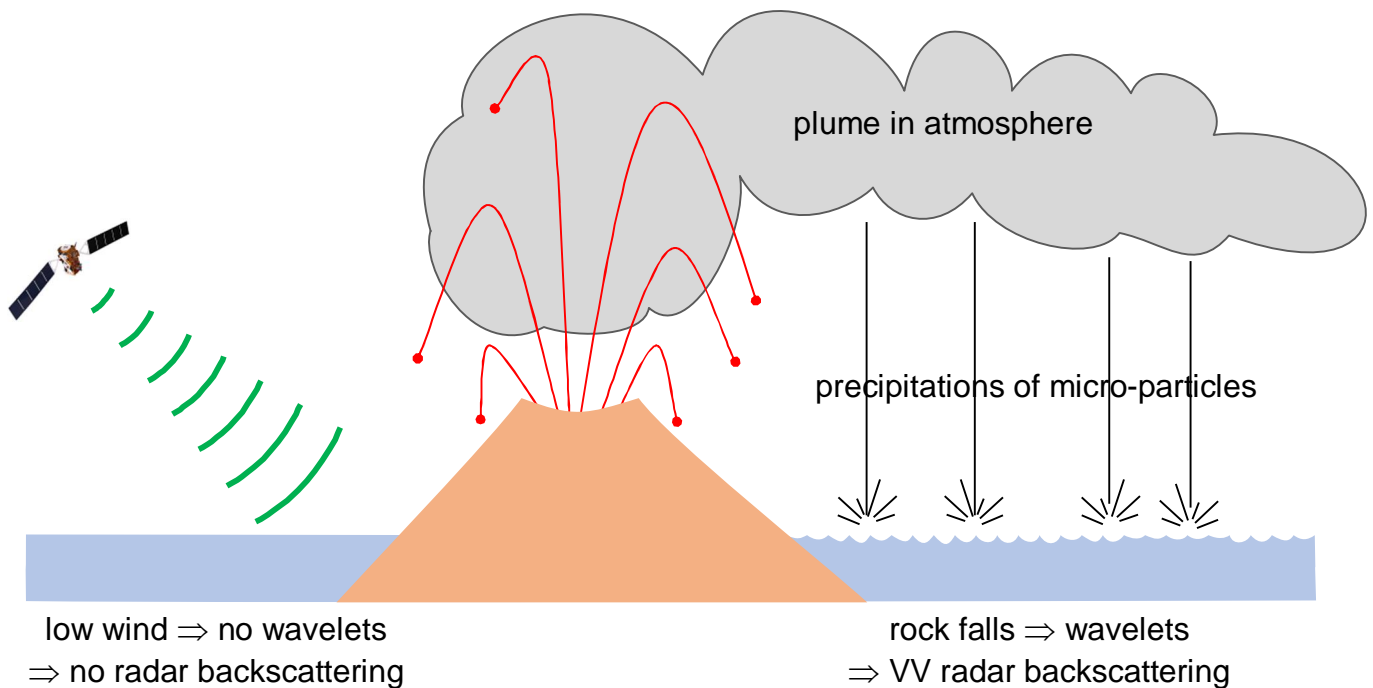


Fig.7: Roughness of the sea detected by the radar signal.



The image acquired on 22 December 2018 (8 hours after the tsunami) also shows concentric waves on the sea surface.

According to Professor Jacques-Marie Bardintzeff and Professor Jean Chorowicz these waves may be a reply of the tsunami but they are concentric to the crater, not to the collapsed area. This should signify that they were generated by the volcanic activity rather than landslides. Distal waves were clearly deviated by coast capes.

Sentinel-1 on 22.12.2018 8 hours after the tsunami Concentric waves

Fig.8: Sentinel-1 acquired on 22 December 2018 - VV,VH,VV colour composition.

[2D animation](#)

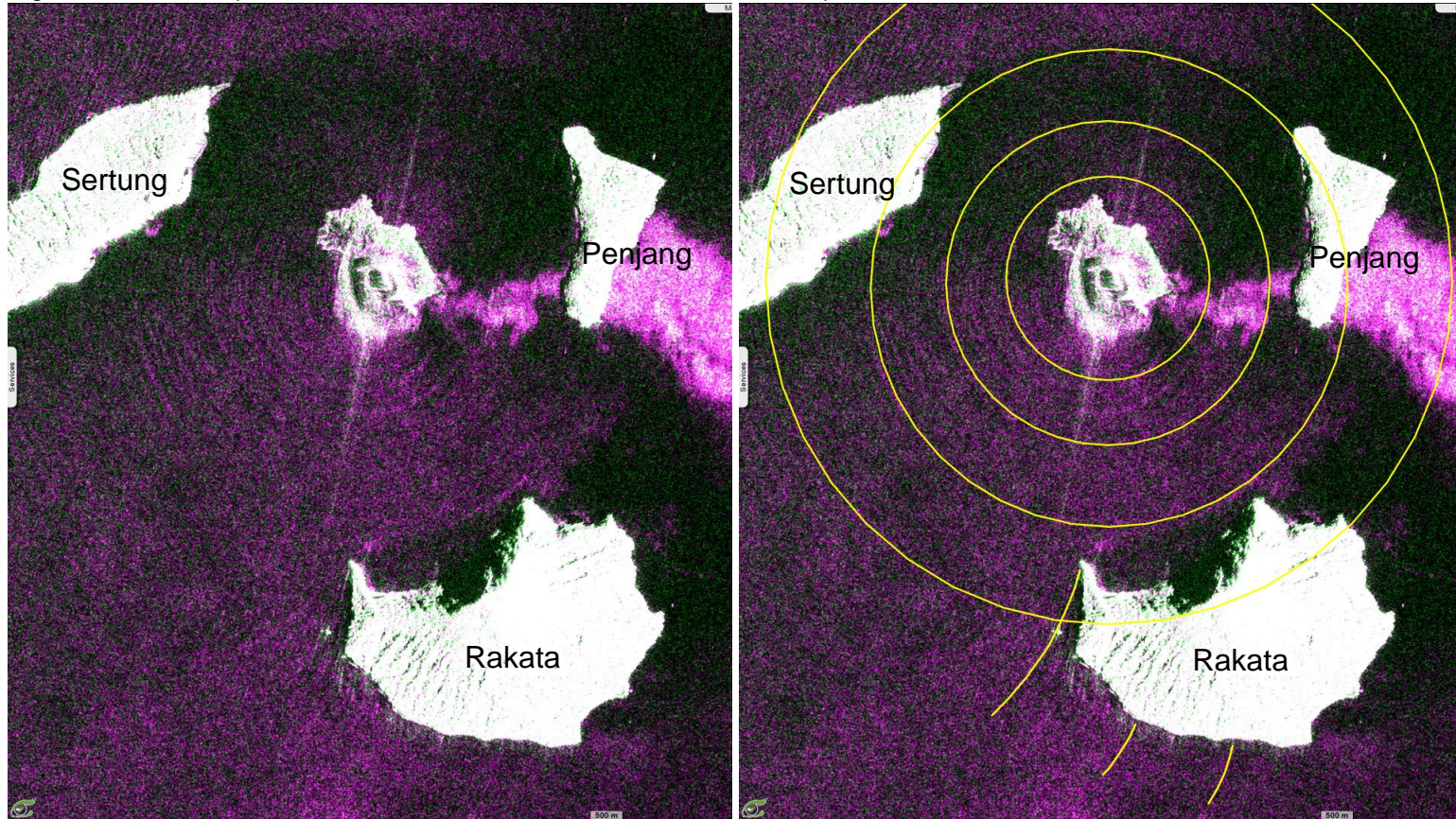
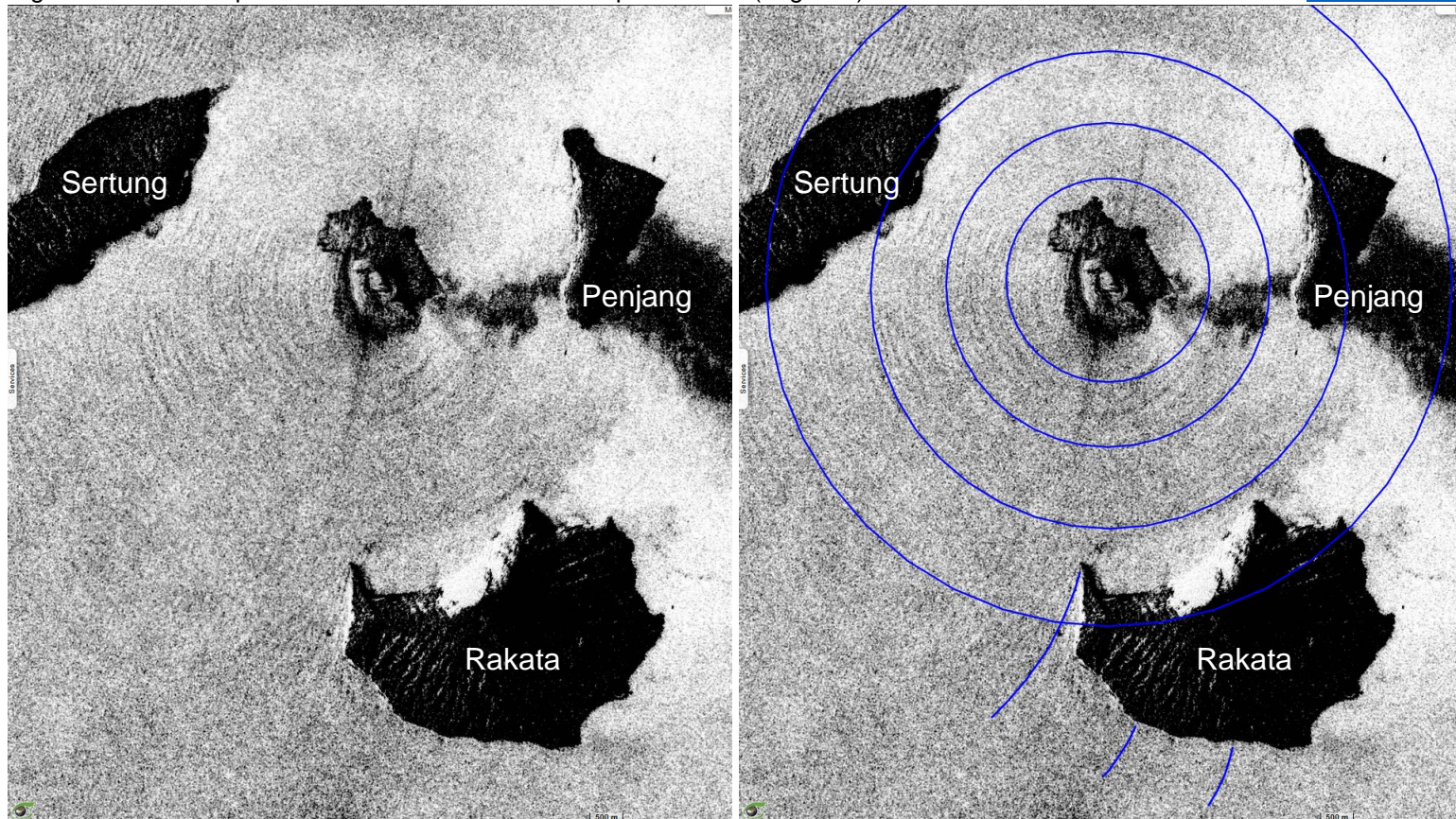


Fig.9: Sentinel-1 acquired on 22 December 2018 - VV polarisation (negative).

[2D animation](#)



This smoke plume may also be observed from [Sentinel-5P](#) satellite and its on-board [TROPOMI](#) (TROPOspheric Monitoring Instrument) that is a low spatial resolution absorption spectrometer operating in the UV, visible, NIR and SWIR domains. Fig.10 shows the level 2A "[Sulphur Dioxide \(SO2\) total column](#)" and fig.11 shows the "[UV Aerosol Index](#)" observed one day before and up to 5 days after the tsunami.

The SO2 emissions (fig.10) reach the maximum in the hours after the tsunami followed by the first eruption (23.12.2018 07:03 UTC). These emissions fade and then a second plume occurs on 26.12.2018 consisting of three clusters. These clusters probably correspond to puffs intermittently released into the atmosphere.

The aerosol emissions (fig.11) do not know these two phases. The observation of the concentration of aerosols is continuous until December 24 and then decreases until disappearing on December 27, 1818.

This 27.12.2018, only persists a small plume of SO2 that will disappear completely the following days (see the animation).

Smoke plume of the volcano

Sentinel-5P - Atmosphere chemistry

SO2 - UV aerosol index

Fig.10: Sentinel-5P / TROPOMI sulphur dioxide (SO2) total column. [2D animation](#)

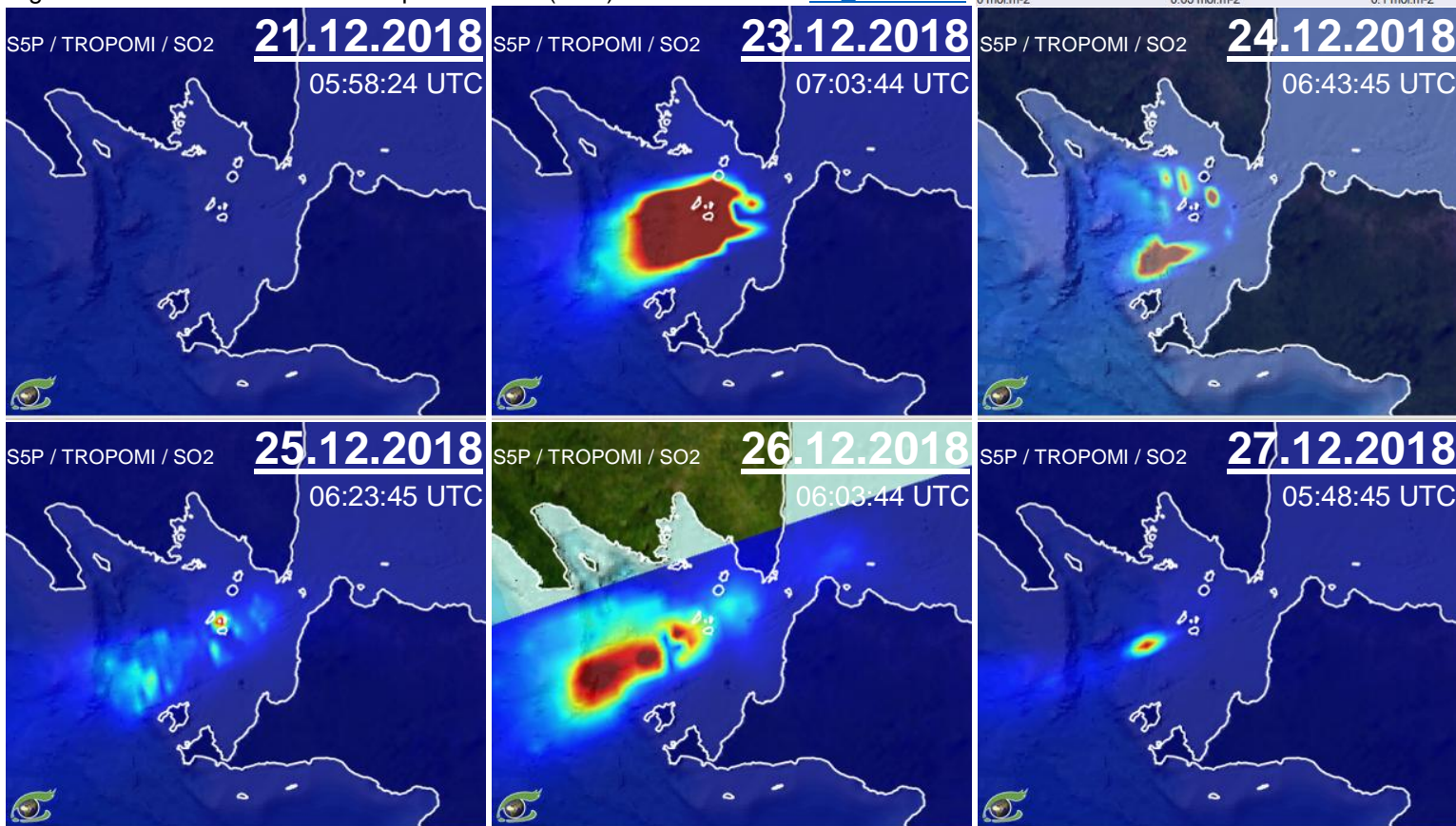
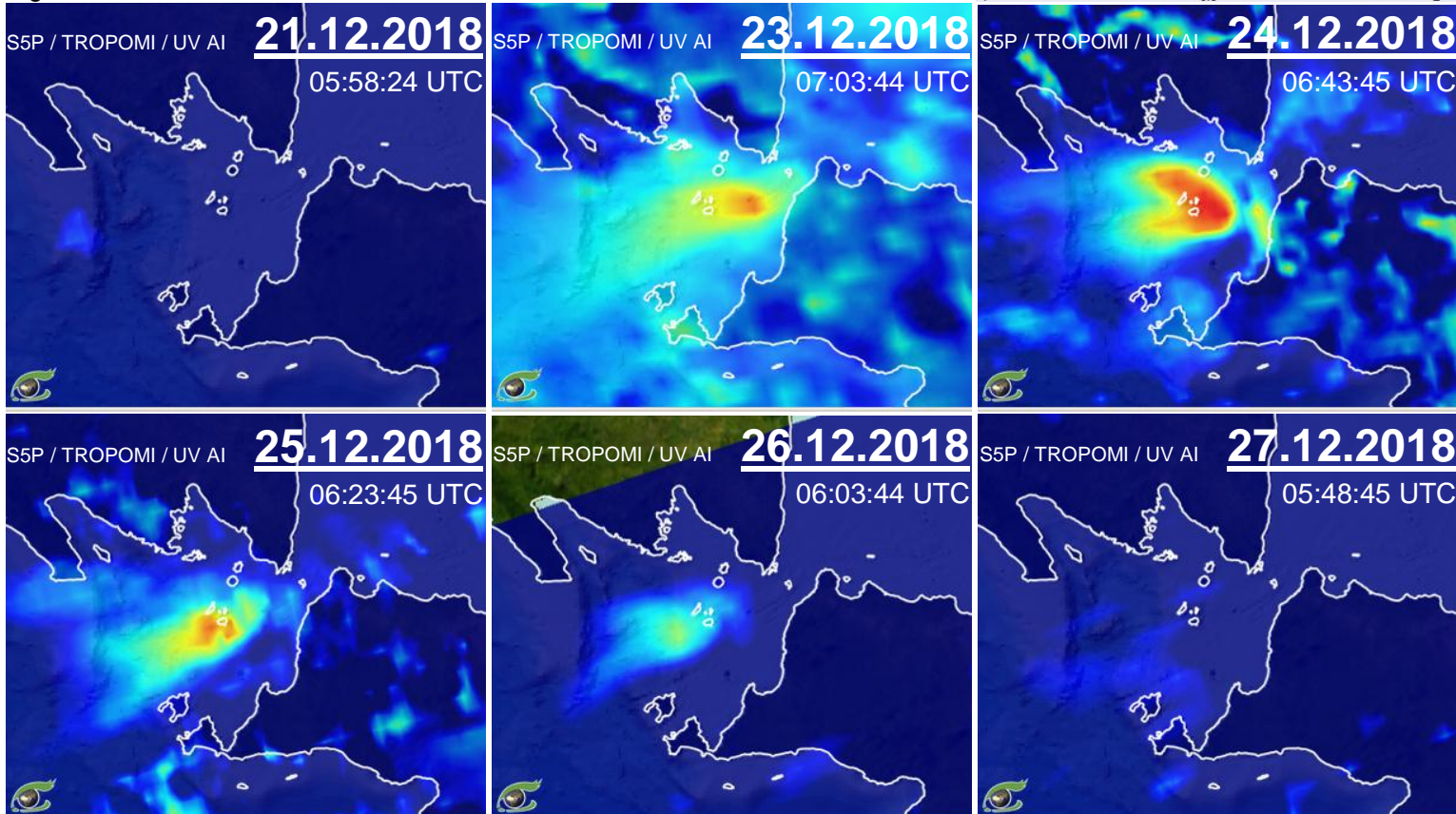


Fig.11: Sentinel-5P / TROPOMI UV Aerosol Index. [2D animation](#)



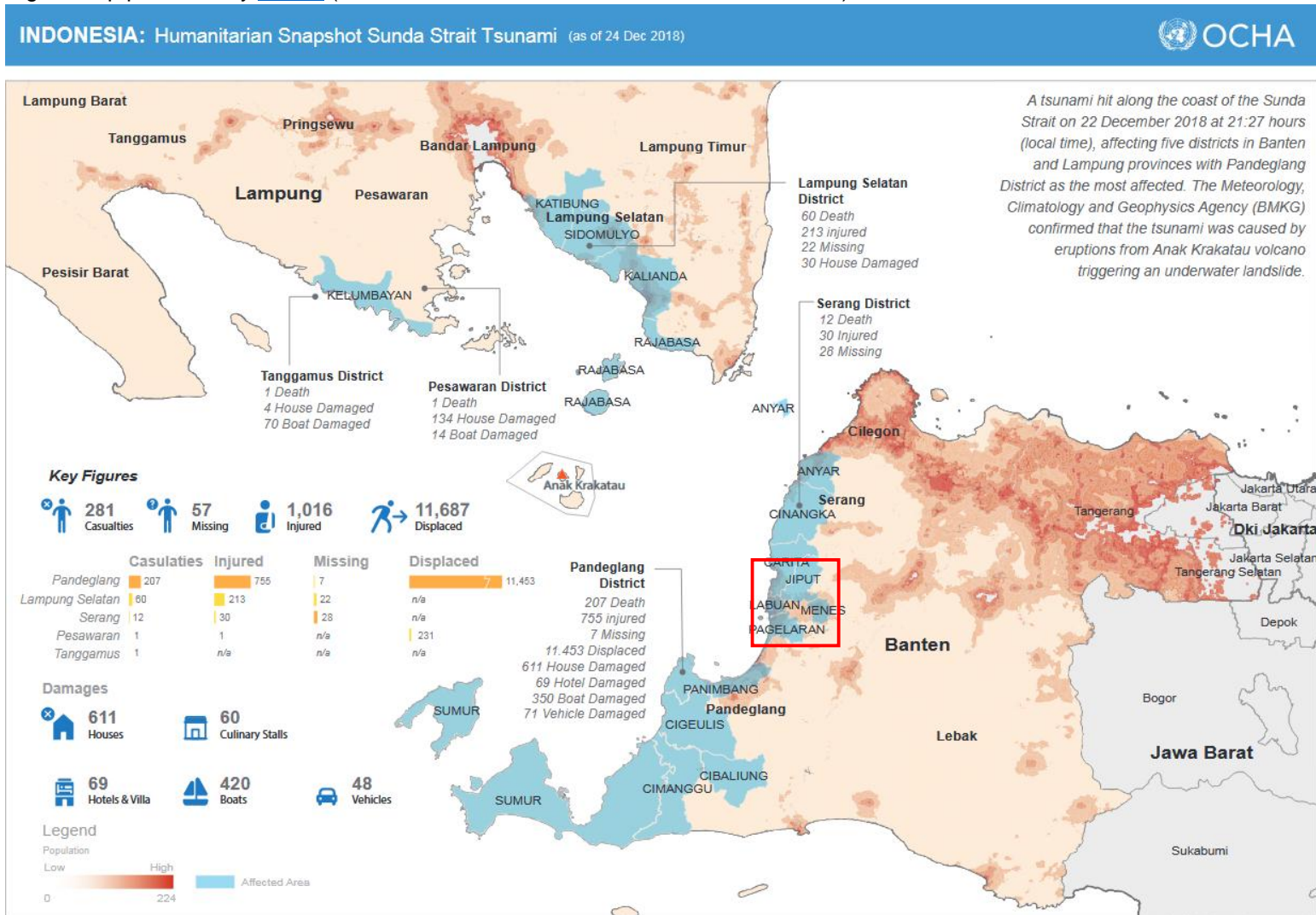
Satellite imagery is particularly useful for managing humanitarian crises. Several organizations have set up portals to share spatial data (non exhaustive list):

- **CMEMS** - European Commission through its JRC agency has activated a "Emergency Management Service" (see [EMSR335](#)).
- **United Nations** - On 24 December 2018, a "[UN News](#)" makes a point of the humanitarian situation (see fig.12).
- **Disaster Charter** - activated on 23 December, a page has been opened with the "[activation ID #594](#)"

The extracts of Sentinel-1 radar images (fig.13) show inland areas (red square in fi.12), displayed in black, which were flooded by the tsunami. Right image (fig.13b) has been acquired on 22.12.2018 at 22:33:45 UTC, i.e. 8 hours after the tsunami.

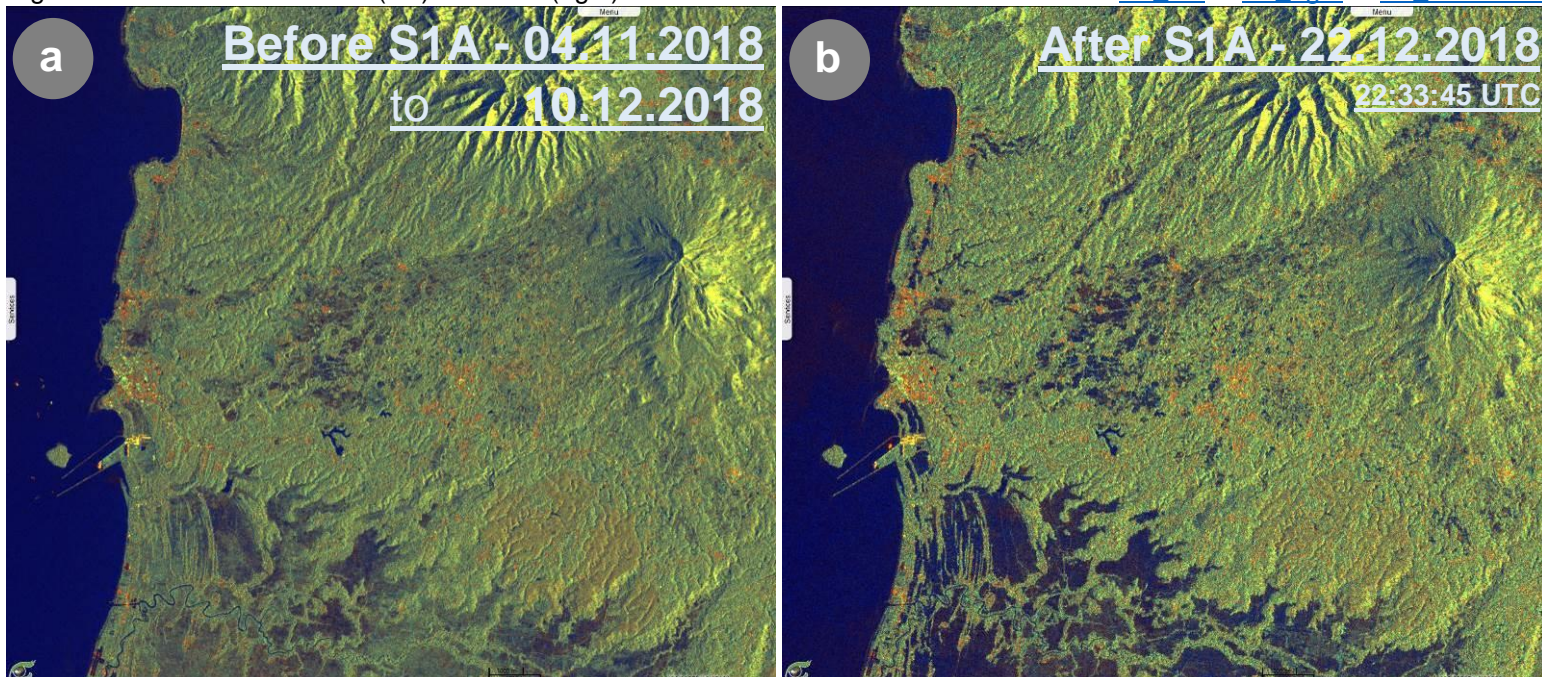
Space imagery for civil protection services and humanitarian organizations

Fig.12 Map produced by [OCHA](#) (Office for the Coordination of Humanitarian Affairs) on 24 December 2018.



The boundaries and names shown and the designations used on this map do not imply official endorsement or acceptance by the United Nations.
 Creation date: 24 Dec 2018 Sources: OCHA, Indonesia Geospatial Agency (BIG), National Disaster Management Agency (BNPb), PVMBG, WorldPop Feedback: ocha-indonesia@un.org www.unocha.org http://humanitarianresponse.info/operations/indonesia www.reliefweb.int

Fig.13: Sentinel-1 radar before (left) and after (right) the tsunami over the west coast of Java. [2D left](#) [2D right](#) [2D animation](#)



VtWeb allows to superimpose in 2D or 3D satellite, meteorological, climatic or biogeophysical data such as some of the geological maps made freely available by the "Commission for the Geological Map of the World" (CGMW) in convention with UNESCO.

The oceanic lithosphere of the Indo-Australia plate subducts at high speed (~7 cm/year) in the NNE direction under the active margin of the Sunda block (Eurasia plate). Subsequent partial in-depth melting in the subducting slab produces magmas that are responsible for a volcanic belt (alignment of orange patches in fig.15) including the Krakatau. Large NE-striking faults in the upper plate between Java-Sumatra and Borneo may ease by places the access of the magma to the surface.

Sentinel-1 over geological maps

Mapping a critical tectonic context

Fig. 14: Sentinel-1 scenes over the geological map of Asia using the geoid altimetry (x10000).

[2D view](#) [3D view](#)

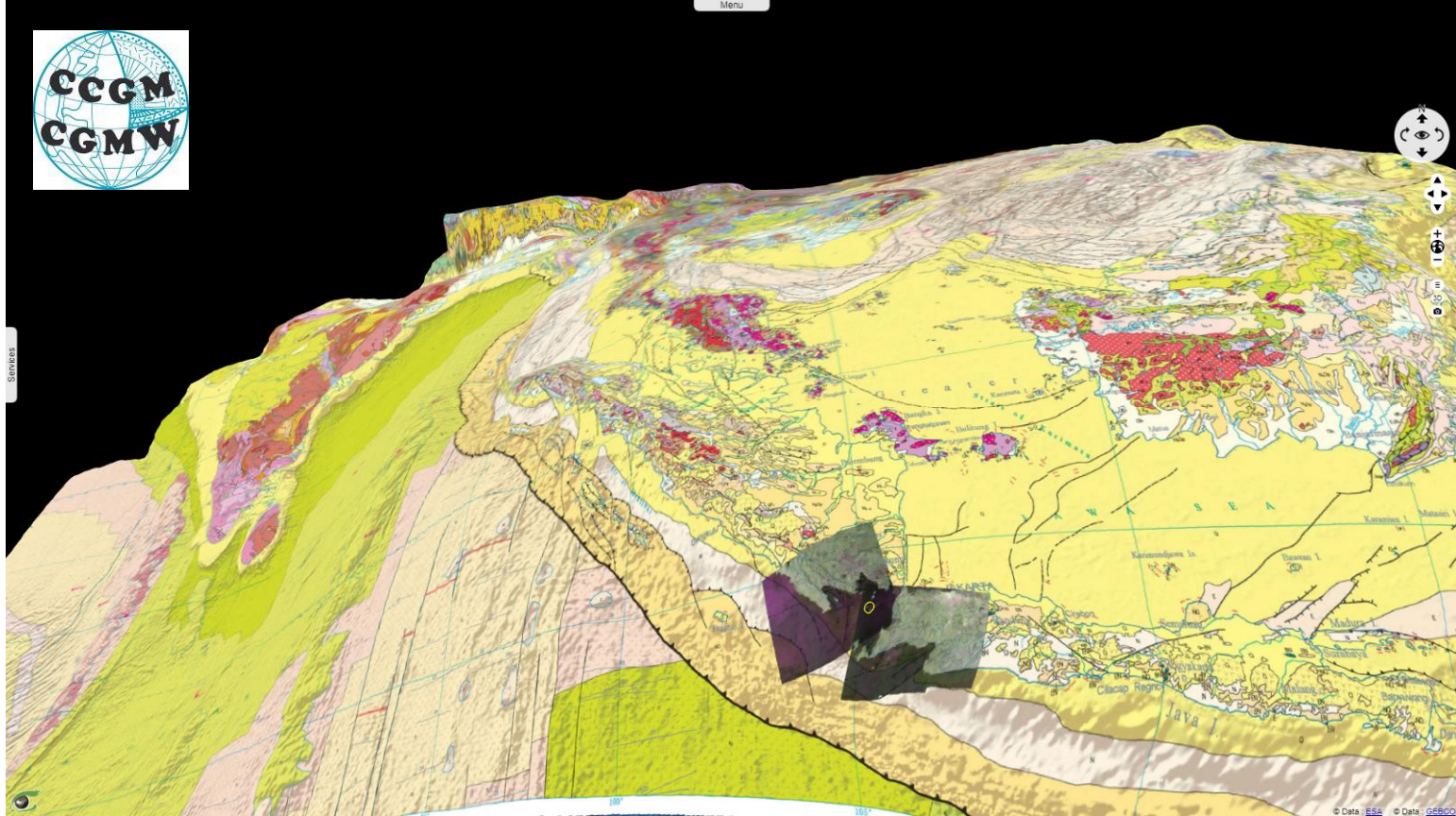


Fig. 15: Sentinel-1 scenes over the West Pacific structural map using the geoid altimetry (x10000).

[2D view](#) [3D view](#)

